Substituted Phosphorous Triazatetrabenzocorroles: Correlation Between Structure and Excited State Properties

Xian-Fu Zhang,[A,B,C] *Yakuan Chang,*[A] *Yanling Peng,*[A] *and Fushi Zhang*[B]

[A]Chemistry Department, Hebei Normal University of Science & Technology,
  Qinhuangdao, Hebei Province, 066004, China.

[B]Chemistry Department, Tsinghua University, Beijing, 100084, China.

[C]Corresponding author. Email: zhangxianfu@tsinghua.org.cn

The photophysical properties of five novel phthalocyanine analogues, dihydroxy phosphorus(v) triazatetrabenzocorrole (PTBC) substituted with $-NO_2$, $-SO_3H$, O^iPr, and $-NH_2$, respectively, were studied by a combination of absorption, steady-state emission, time-resolved fluorescence, and laser flash photolysis. All substituents, even for the strong electron-donating $-NH_2$, cause only a slight red shift of their absorption and emission maxima. These complexes are generally monomeric in organic solution, whereas the sulfonated derivative, $PTBC(SO_3H)_4$, slightly aggregates in aqueous buffer. Distinct from phthalocyanines, PTBCs substituted with $-NO_2$ or $-NH_2$ still show high photo activities. The electron-withdrawing $-NO_2$ and $-SO_3H$ decrease the fluorescence quantum yield but increase the triplet formation yield to 0.76 and 0.82, respectively. All PTBCs have long triplet lifetimes and hence generate singlet oxygen efficiently with a quantum yield from 0.43 to 0.75. Together with the ground-state absorption properties, the results suggest that these PTBCs may be used as excellent photosensitizers for photodynamic therapy.

Introduction

Triazatetrabenzocorrole (TBC) is a π-extended corrolazine derived from corrole (Fig. 1). Corroles, however, are π-contracted porphyrins in that they are missing one meso-nitrogen but still retain the aromatic, tetrapyrrolic structure. Corroles have only received much attention as of this century because of the recent discoveries of facile methodologies for their synthesis.[1–5] TBC is also a π-contracted phthalocyanine (PC), and was first obtained by PC reduction in 1981.[6] The structure of TBC and its complexes (TBCs), therefore, has similarities to corrole, porphyrin, and PC. The properties of TBCs are, therefore, expected to inherit the features of corroles, porphyrins, and PCs.

Corroles show a high ability to stabilize high-valent oxidation states, for example, Fe^{IV}, Co^V, and even Mn^{VII} corroles are thermally stable, which is one of the most fascinating properties of these ligands. Similar to corroles, TBCs exhibit low oxidation potentials and high reduction potentials. The optical property of TBCs in the red region, however, shows inherited attributes of PCs, i.e., a strong Q band (around 650 nm), whereas in the UV region it is more like that of porphyrin, i.e., a Soret band (∼440 nm) that is even stronger than its Q band. These combined merits make TBCs attractive for several potential applications, for example, as excellent electron donors and sun light antennas in dye-sensitized solar cells, photo-medicine in photodynamic therapy (PDT) of tumours, and blue-laser applications, etc.

Phosphorous TBC (PTBC), as displayed in Fig. 2, was first reported by Gouterman in 1981[6] and is among the few TBC complexes (Si, Ge, Sn) synthesized so far.[7] The central P^V is
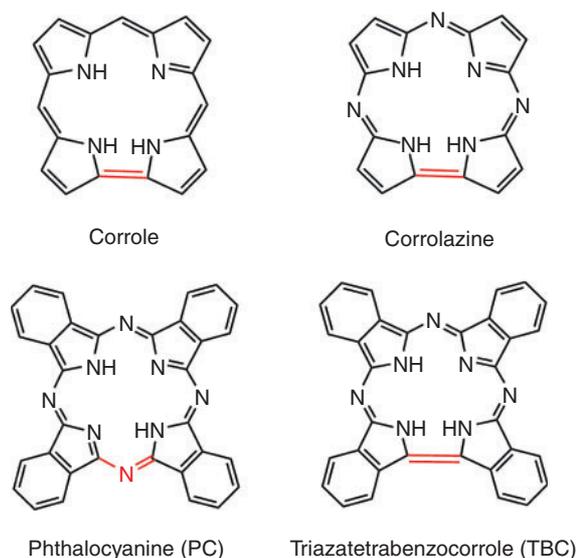

Fig. 1. The chemical structure of corrole, corrolazine, phthalocyanine, and triazatetrabenzocorrole.

stabilized by its corrole structure. The accurate structure and basic properties were later elucidated by the groups of Liu,[8–10] Li,[11,12] and Fox.[13] The sulfonated PTBC was shown to be photoactive for DNA cleavage.[14] In spite of these reports, the synthesis and properties of TBCs have remained largely unexplored, which is surprising given the importance of PCs and
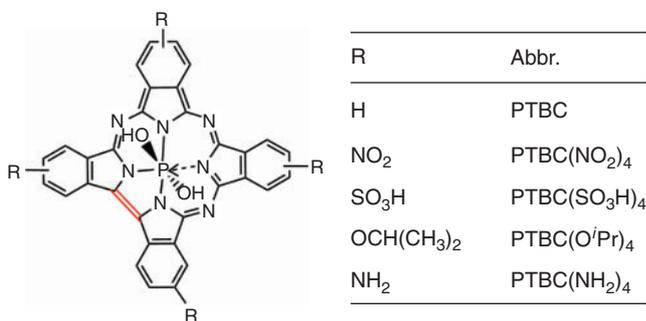
Fig. 2. Chemical structure of PTBCR$_4$.

Fig. 3. The typical UV-Vis spectra of PTBCR$_4$ in DMF (normalized for comparison), the spectra for PTBC(O^{i}Pr)$_4$ and PTBC(SO$_3$H)$_4$ are not included because they are almost indistinguishable from that of phosphorus(v) triazatetrabenzocorrole.

their analogues in the electronic, environmental, and health care fields.

Most potential applications of TBCs or PCs are based on their photophysical properties, and structural optimization is usually desirable for this purpose. We, therefore, prepared PTBCs bearing typical organic groups to relate their excited state properties and structures.

Results and Discussion

Ground State Absorption Spectra

The UV-vis absorption spectra of the PTBCs were measured in *N,N*-dimethylformamide (DMF). Typical spectra are displayed in Fig. 3 for comparison. Each spectrum contains a Q band with three noticeable peaks from 580 to 700 nm and a stronger Soret band at around 440 nm. The spectra of PTBC(O^{i}Pr)$_4$ and PTBC(SO$_3$H)$_4$ are almost indistinguishable from that of PTBC. Each substituent, whether it is an electron-donating or with-drawing group, causes a red shift in its absorption maximum compared with that of PTBC. Amino substitutions gave the largest bathochromic shift, which is 14 nm, and also cause the broadening of absorption bands and hence the disappearance of Q-band splitting, which is common to many chromophores bearing NH$_2$. The shift is 2 nm for –O^{i}Pr, 4 nm for –SO$_3$H, and 6 nm for –NO$_2$, which are all relatively small. The missing *meso*-nitrogen causes the direct linkage of two crowded pyrroles. As a result, the steric strain in PTBCs is significantly higher than that in PCs. This type of steric strain generally causes a hypso-chromic shift,[15] which, therefore, explains the blue-shifted absorption maximum of PTBCR$_4$ compared with that of the corresponding PCR$_4$. In the particular case of TBCs, the steric strain also induces the deformation of the planar structure in PCs to the domed shape of TBCs, as shown by the crystal structure of SiTBC.[16] This is probably part of the reason that the substituents of PTBC exert less effects.

Four different structures have been proposed in the literature for PTBCs,[8,10,11,13] as shown in Fig. 4. The difference between them is the valency and binding status of phosphorous. The early proposals (structure II and III) were mainly based on the mass spectra.[8,11] Matrix-assisted laser desorption–ionization time-of-flight (MALDI-TOF) mass spectrometry nowadays provides more accurate *m/z* and suggested recently that I and IV are the more possible choices.[10,13] Our data is consistent with structure IV based on our mass and NMR spectra, and the effect of solvent polarity on UV-vis as described in the following.

The small red-shift caused by the substituents also provides other important structural information, i.e., the ionic structure should be excluded, otherwise the π cation of PTBC (electron poor) will strongly interact with NH$_2$ (electron rich) and show
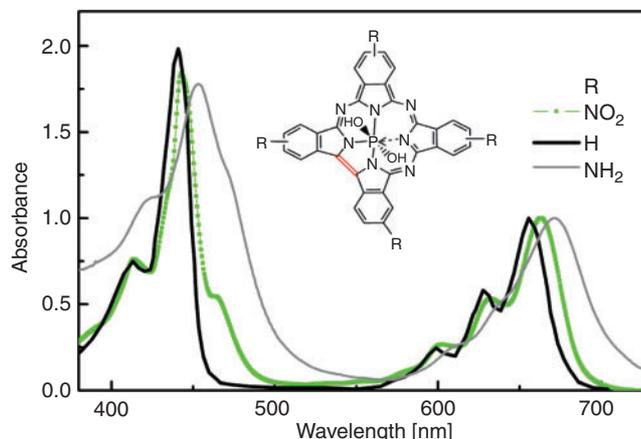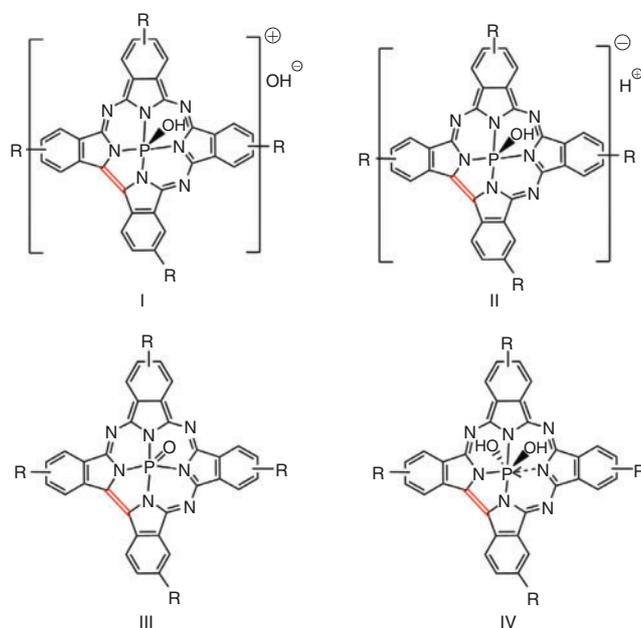

Fig. 4. Proposed structures for phosphorus(v) triazatetrabenzocorroles.

a very large substitution effect.[15] This conclusion is further supported by the solvent effect in the following.

Solvent Effect on Absorption Spectra

PTBC(O^{i}Pr)$_4$ was selected to study the effect of solvent polarity on its absorption spectrum because of its good solubility in both polar and non-polar solvents. If the aromatic ring of the TBCs is indeed positively charged, an intra-molecular donor–acceptor (D–A) system will be formed for PTBC(NH$_2$)$_4$ and PTBC(O^{i}Pr)$_4$ in which –NH$_2$ or –O^{i}Pr groups act as donors. It is well established that a D–A molecule shows a very large dependence of λ_{max} on solvent polarity.[17] The λ_{max} of PTBC(O^{i}Pr)$_4$ in different solvents are plotted against $E_T(30)$, an empirical parameter of solvent polarity values,[17] and shown in Fig. 5. Two trends can be found from Fig. 5. (1) The solvent effect is quite small, from non-plgar benzene (666 nm) to highly polar acetonitrile (652 nm), the change of λ_{max} is only 14 nm, which is of a level that is comparable only to a non-polar compound,
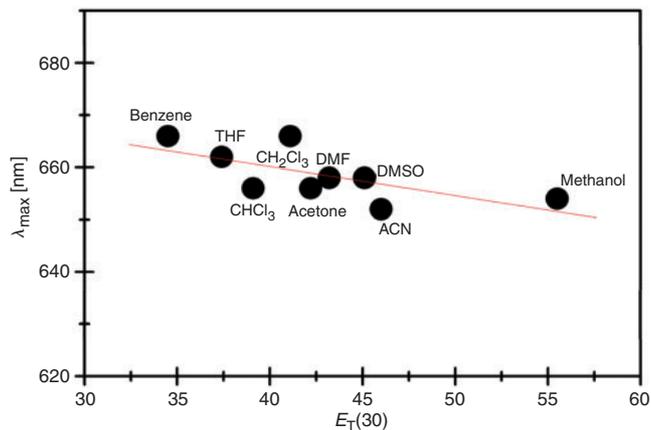
Fig. 5. Effect of solvent polarity on the absorption maximum of PTBC(O^{i}Pr)$_4$.

such as C$_{60}$. (2) An increase in polarity causes the blue shift of λ_{max}, i.e., a negative solvatochromism. Therefore, the HOMO of TBC(O^{i}Pr)$_4$ is stabilized by a non-polar solvent. Both of the facts suggest that highly dipolar or zwitterionic electronic ground state I and II should not be the real structure of TBC(O^{i}Pr)$_4$.

Absorption and Aggregation

Many organic dyes show a tendency of self-aggregation even at a concentration as low as 10^{-6} mol dm^{-3} in aqueous solution.[18] Some PCs can form H-type dimers through the equilibrium: $2 \times$ monomer $\leftrightarrows$ dimer.[18] The presence of H-dimers, which are known to be non-photoactive, lowers the effective concentration of photoactive monomer and hence reduces the photosensitizing ability. The water-soluble sulfonated derivative of PTBC was, therefore, chosen to study the aggregation behaviour. The presence of H-dimer or higher aggregates often show blue-shifted new bands in the UV/vis absorption spectra. Fig. 6 compares the absorption spectra of PTBC(SO$_3$H)$_4$ in DMF and aqueous Tris buffer (pH 7.4). The shape of the spectrum in aqueous solution was obviously changed, the peak position was blue-shifted to 640 nm and the shoulder at 625 nm was raised markedly, which indicates the appearance of a new band. The absorbance at 630 nm was plotted against its concentration (inset of Fig. 6). The deviation from Beer's law in aqueous buffer is obvious, which also suggests that aggregates were formed. Assuming that only dimer is present, the dimerization constant was evaluated to be 0.65 ($\pm$ 0.24) $\times 10^5$ mol^{-1} dm^3 by using our reported method.[18] This constant is one order smaller than that of sulfonated PCs, such as 0.56×10^6 mol^{-1} dm^3 for tetrasulfonated chloroaluminum phthalocyanine and 1.0×10^6 mol^{-1} dm^3 for tetrasulfonated zinc phthalocyanine. This significantly lower tendency of aggregation is probably a result of the larger difficulty of PTBC to approach each other, because the oxophosphorous is out of the dome-shaped π system.

Steady State Fluorescence

Fig. 7 presents a typical fluorescence spectra excited at 615 nm, together with the absorption spectra. The effect of substitution on the emission maximum is similar to the case of the absorption spectra. Complete data are collected in Table 1. The most noticeable effect is the very small stokes shift ($\Delta \nu$) for all PTBCR$_4$, which is 5.4 nm on average. This small $\Delta \nu$ indicates that the difference of dipole moments between the excited state and ground state is also small, owing to the rigid structure of the fluorophore.
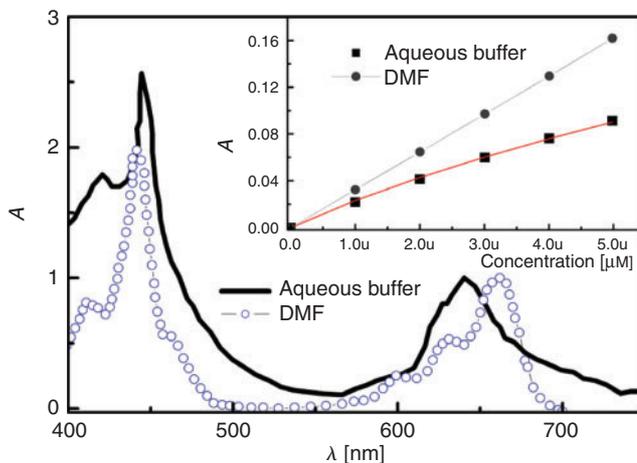

Fig. 6. Comparison of absorption spectra of PTBC(SO$_3$H)$_4$ in DMF and aqueous buffer (pH 7.4), spectra were normalized at Q band maximum for viewing clearly. Inset is the plot of absorbance against concentration.
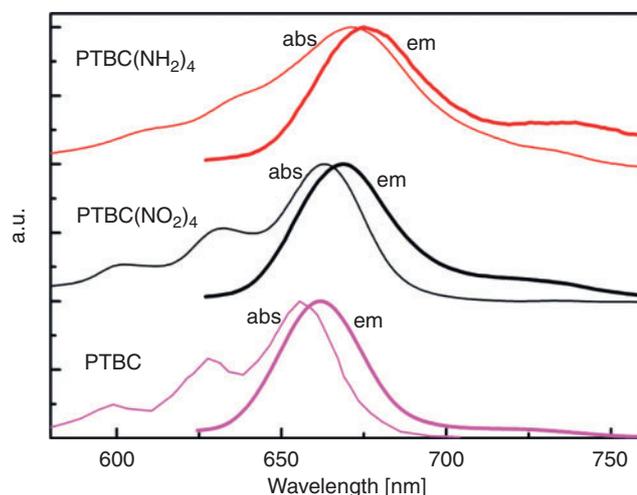

Fig. 7. Normalized fluorescence and absorption spectra in DMF. Excitation wavelength is 615 nm, the absorbance at the wavelength was adjusted to be 0.09.

The rigidity is imposed by the loss of one nitrogen atom, which brings two isoindoles closer in PTBCs than that in PCs. The mirror-image symmetry between the fluorescence and absorption spectra does not seem to hold in PTBCR$_4$ as seen from Fig. 7.

All PTBCs fluoresce moderately in DMF, although the electron-withdrawing groups –NO$_2$ and –SO$_3$H lower the fluorescence quantum yield (Φ_F) by 36% and 58%. –O^{i}Pr and –NH$_2$, however, show no marked effect on Φ_F. The presence of –NO$_2$ or –SO$_3$H in an aromatic fluorophore usually enhances the intersystem crossing from S$_1$ (lowest singlet excited state) to its T$_1$ (lowest triplet state) and hence decreases Φ_F.[15]

Typical fluorescence decay profiles in DMF are shown in Fig. 8. Fitting the data biexponentially gave satisfactory results with χ^2 less than 1.10, and the percentage of major components varies from 94 to 96%. The S$_1$ lifetime (τ_f) of the major components falls in the range from the shortest of 2.21 ns for PTBC(SO$_3$H)$_4$ to the longest of 4.29 ns for PTBC(O^{i}Pr)$_4$. The minor components ($\sim$5%), however, all show a much longer τ_f between 10 and 15 ns. The presence of minor components might reflect the contribution from: (1) four possible regioisomers and

Table 1. Photophysical parameters of PTBC(R)$_4$ in DMF

Parameter	R				
	–NO$_2$	–SO$_3$H	–H	–O^{i}Pr	–NH$_2$
λ_{max}, abs [nm]	662	660	656	658	670
λ_{max}, em [nm]	669	662	664	663	675
Stokes shift [nm]	7	2	8	5	5
log ε [M^{-1} cm^{-1}]	4.25	4.34	4.41	4.69	4.51
E_S [eV]	1.87	1.87	1.88	1.88	1.85
τ_f [ns]	2.8	2.21	3.3	4.29	3.2
Φ_f	0.23	0.15	0.36	0.41	0.34
k_f ($\times 10^9$) [s^{-1}]	0.082	0.068	0.109	0.096	0.106
λ_{T-T} [nm]	490	500	480	490	500
log ε_T [M^{-1} cm^{-1}]	3.82	3.94	3.95	4.21	4.09
Φ_T	0.76	0.82	0.45	0.48	0.59
k_{isc} ($\times 10^9$) [s^{-1}]	0.271	0.371	0.136	0.112	0.184
τ_T [μs]	124	232	95	75	106
Φ_Δ	0.75	0.72	0.43	0.44	0.54

(2) a small amount of III as mentioned earlier. However, the signal of the minor component is too weak to be conclusive.

The radiation rate constant k_f, obtained by Φ_f/τ_f, shows no significant change with substituents.

Nanosecond Transient Absorption Spectra and Kinetics

The transient absorption spectra of PTBCR$_4$ were recorded in argon-saturated solutions in DMF ($\sim 10 \times 10^{-6}$ M). The samples were excited using Nd:YAG laser pulses (7 ns, 3 mJ) at 355 nm, and spectra were recorded point by point over the wavelength range 350–800 nm in 10 nm steps. The time dependent transient absorption data are displayed in Fig. 9 along with a representative decay profile (Fig. 9, inset). All PTBCR$_4$ showed similar absorption features, such as a negative absorption (bleaching) in the Q and Soret band regions, and a broad positive absorption feature centred near 490 nm. Taking PTBC(O^{i}Pr)$_4$ as an example, isosbestic points were detected between the Q-band bleaching and the positive feature to the red side (near 410 nm and 580 nm). Under conditions of argon saturation, the negative and positive absorption decayed to the prepulse baseline in accord with an exponential rate law. The absorption at 380 and 480 nm and bleaching kinetics had identical lifetimes (τ_T) of 75 μs for PTBC(O^{i}Pr)$_4$.

In the presence of oxygen, the transient absorbance of 500 nm decayed exponentially to a zero baseline with a much faster rate, and the τ_T of PTBC(O^{i}Pr)$_4$ was reduced to 0.45 μs. The bimolecular rate constant for oxygen quenching could be evaluated to be 1.0×10^9 M^{-1} s^{-1}, which is similar to that for the exergonic energy transfer from most triplet states to oxygen with rate constants in the order of 10^9 M^{-1} s^{-1}.

The positive absorption near 490 nm and 380 nm can be assigned to the triplet–triplet (T$_1$–T$_n$) absorption by analogy to that of PCs. The appearance of the isosbestic points between positive absorption and ground state bleaching indicated that the species near 490 nm are responsible for the ground state repopulation without any intermediate entities.

The values of the triplet absorption coefficient (ε_T) and triplet state quantum yields (Φ_T) are collected in Table 1. ε_T for all PTBCs are close, but the triplet state lifetime and the triplet quantum yield seem to increase with substitution. The presence of –NO$_2$ and –SO$_3$H, in particular, enhance the intersystem crossing and increase Φ_T significantly.
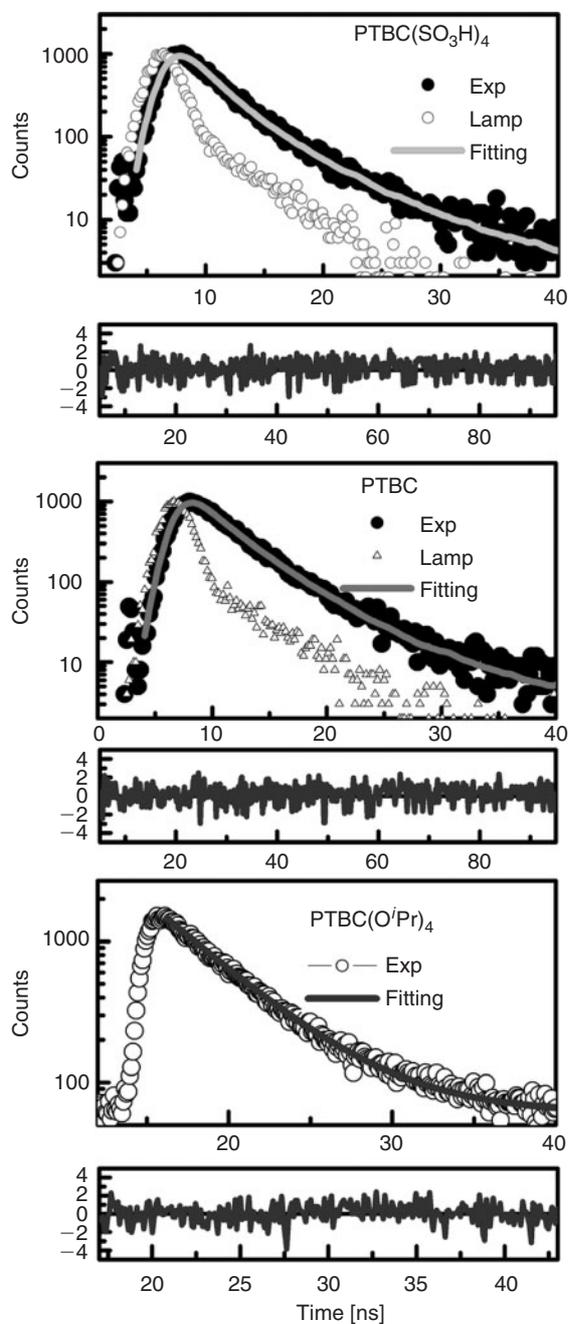

Fig. 8. Time profile for fluorescence decay of phosphorus(v) triazatetrabenzocorrole (PTBCs) in DMF. Excitation is at 650 nm with absorbance 0.20 and emission is at 700 nm. PTBC(O^{i}Pr)$_4$ was excited by a 100 ps diode laser, whereas PTBC and PTBC(SO$_3$H)$_4$ were excited by a nanosecond hydrogen flash lamp.

Singlet Oxygen Generation

Singlet oxygen quantum yields (Φ_Δ) were determined in DMF using diphenylbenzofuran (DPBF) as a chemical trapper and ZnPc as the reference as described in the experimental section. The irradiation wavelength was 670 nm. The disappearance of DBPF was monitored using a UV/Vis spectrometer at 415 nm. The reaction time was controlled to be no longer than the first 5 min so that no appreciable amount of a sensitizer was photobleached. The reactions are all first order in nature from the linear reaction kinetics. Φ_Δ were then obtained from the slope of the linear equation, the values vary from 0.43 to 0.75, which
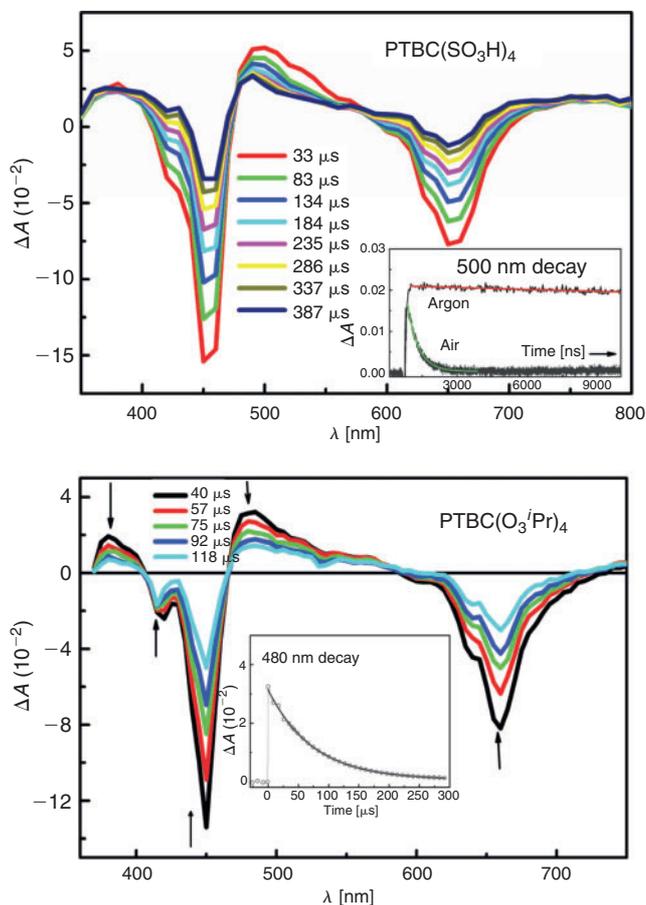
Fig. 9. Transient absorption spectra in argon-saturated DMF with laser excited at 355 nm. Inset shows the decay of absorbance at the given wavelength. PTBC, phosphorous triazatetrabenzocorrole.

indicates that they are all fairly good sensitizers for singlet oxygen generation. Each of them has a Φ_Δ that is close to but slightly smaller than the corresponding Φ_T. This relationship is rationalized by Eqn 1.[18]

$$\Phi_\Delta = \Phi_T \frac{k_{et}[O_2]}{\tau_T^{-1} + k_{et}[O_2]/\eta}, \qquad (1)$$

in which k_{et} is the rate constant for energy transfer from a triplet state to oxygen and η is the efficiency of the transfer that forms singlet oxygen. k_{et} is in the order of $10^9\,M^{-1}\,s^{-1}$ and $[O_2]$ is $\sim 2.0 \times 10^{-3}\,mol\,dm^{-3}$. Φ_Δ is mainly determined by Φ_T, τ_T, and k_{et}. Because the triplet lifetime is so long such that $\tau_T^{-1} << k_{et}[O_2] < k_{et}[O_2]/\eta$, hence $\Phi_\Delta = \Phi_T\eta$, and η is close to unity.

Conclusions

Five dihydroxy phosphorus(v) triazatetrabenzocorroles substituted with –NO_2, –SO_3H, –H, –O^iPr, and –NH_2 respectively, were prepared to study the photophysical properties of the novel macrocyclic compounds. These complexes are generally monomeric in organic solution, whereas the sulfonated derivative, PTBC(SO_3H)$_4$, only slightly aggregates in aqueous buffer. Both strong electron-donating and electron-releasing substituents show only a slight effect on their emission and absorption maxima owing to the non-planar structure of PTBCs. Distinct from phthalocyanines, PTBCs substituted with –NO_2 or

–NH_2 still show high photoactivities. The fluorescence quantum yield is lowered appreciably together with a significant concurrent increase of triplet formation yield when electron-donating –NO_2 and –SO_3H are introduced into PTBC's aromatic ring. All PTBCR$_4$ have a long triplet lifetime and good singlet oxygen quantum yield from 0.43 to 0.75. Together with the ground-state absorption properties, the result suggests that they may be used as an excellent photosensitizer for PDT.

Experimental

Materials

Zinc phthalocyanine (ZnPc) and metal-free phthalocyanine (H$_2$Pc) were purchased from Tokyo Kaise. The synthesis of H$_2$Pc(β-NO_2)$_4$ (metal free tetra(β-nitro)phthalocyanine), H$_2$Pc (β-O^iPr)$_4$ (metal free tetra(β-isopropyloxy)phthalocyanine), H$_2$Pc(β-SO_3H)$_4$, and H$_2$Pc(β-NH_2)$_4$ were previously reported.[19] All other reagents for synthesis were of analytical grade and used as received, solvents were generally dried and freshly distilled before use.

Synthesis

^{1}H NMR spectra were obtained using a Bruker AMX 400 MHz NMR spectrometer. FT-IR spectra (KBr pellets) were recorded on a Perkin–Elmer spectrum 2000 FT-IR spectrometer. Mass spectrometry data was recorded on a BIFLEXIII MALDI-TOF Mass instrument. Ground-state electronic absorption spectra were recorded on either a HP8452A or a Hitachi 4500 UV/Vis spectrophotometer.

PTBC

PTBC was prepared from H$_2$Pc according to the literature.[11] The procedure is also general for others as follows: 0.6 g of H$_2$Pc (1.17 mmol) in 10 mL of pyridine was added into a 50 mL three-necked round-bottomed flask, which was equipped with a reflux condenser and a gas inlet tube. Pyridine (5 mL) that contained 3.2 mL of PBr$_3$ (35 mmol) was then added and the resulting mixture was heated at 90–100°C under stirring for 2 h. After cooling, the mixture was poured into water and filtered, the solid was washed thoroughly with water. The crude product was dissolved in pyridine and purified by column chromatography on neutral alumina using pyridine/ethanol (1/1) as eluent. Yield: 51%. ν_{max}(KBr)/cm^{-1} 3460 (PO-H), 3072, 1614, 1578, 1525 (C=N), 1478, 1425, 1361, 1343, 1296, 1261, 1118, 1102, 982 (P-OH), 832, 761, 714, 638. δ_H (D$_5$-pyridine) 8.13–8.28 (m, 8H), 9.39–9.61 (m, 8H). δ_P (D$_5$-pyridine) −200.70. m/z (MALDI-TOF) 564.21 [M$^+$].

PTBC(O^{i}Pr)$_4$

This was prepared from H$_2$Pc(O^{i}Pr)$_4$ according to refs [8,11]. Chloroform/pyridine was used as the eluent to purify the product. Yield: 47%. ν_{max} (KBr)/cm^{-1} 3457 (PO–H), 1613 (C–C), 1522 (C=N), 1358, 1235 (R–O–Ar), 1105, 980 (P–OH), 825. δ_H ((CD$_3$)$_2$SO) 8.51–9.63 (m, 4H, Ar-H), 7.18–7.92 (m, 8H, Ar-H), 3.90–5.42 (m, 4H, CH-O), 3.31 (s, 2H, PO-H), 1.31–1.72 (d, 24H,CH$_3$). δ_P ((CD$_3$)$_2$SO) −202.81. m/z (MALDI-TOF) 777.28 [M$^+$].

PTBC(NO$_2$)$_4$

This was prepared from H$_2$Pc(NO$_2$)$_4$ according to the general procedure.[8,11] Pyridine was used as the eluent to purify the product. Yield: 39%. ν_{max} (KBr)/cm^{-1} 3430 (PO–H), 1613, 1579, 1525 (C=N), 1489, 1354, 1100, 980 (P–OH), 817, 754,

682. δ_H (D$_5$-pyridine) 8.8–9.6 (m, 4H, Ar-H), 7.3–8.0 (m, 8H, Ar-H). m/z (MALDI-TOF) 744.13 [M$^+$].

PTBC(NH$_2$)$_4$

This was prepared from PTBC(NO$_2$)$_4$ by using Na$_2$S as a reducing agent according to the reported procedure.[19] Water (20 mL) that contained 0.10 g of PTBC(NO$_2$)$_4$ and 10 g of Na$_2$S·9H$_2$O was stirred at 60°C under nitrogen for 24 h. The resulting suspension was filtered off and washed. The obtained solid was boiled in 20 mL of 1.0 M HCl for 0.5 h and filtered off. The resulting solid was then added to 20 mL of 1.0 M NaOH and stirred for 1 h at room temperature, and then filtered off and washed to neutral. The acid/base treatment was repeated twice before drying the solid. Yield: 58%. ν_{max} (KBr)/cm^{-1} 3430, 1613, 1489, 1354, 1100, 817, 754, 682. m/z (MALDI-TOF) 624.13 [M$^+$]. (Found: C 64.0, H 2.9, N 26.3. Calc. for C$_{32}$H$_{20}$N$_{11}$OP: C 63.5, H 3.3, N 25.5.)

PTBC(SO$_3$H)$_4$

PTBC (0.2 g, 0.36 mmol) was dissolved in 5 mL of chlorosulfuric acid and stirred at 130°C for 6 h under nitrogen. After cooling to 85°C, 1.0 mL of SOCl$_2$ was added and stirred for another 4 h. The mixture was subsequently poured into ice, and the resulting precipitate was filtered off and washed with cold water. The product was then dissolved in 5 mL of 98% sulfuric acid and precipitated by pouring into ice for filtering. This purification procedure was repeated twice before drying. The product was washed with distilled cold water and dried under vacuum. Yield: 43%. ν_{max} (KBr)/cm^{-1} 3389 (P–OH), 1626 (C=C), 1577 (C=N), 1384, 1279, 1236–1122 (SO$_2$), 1076, 749. δ_H ((CD$_3$)$_2$SO) 11.02–11.33 (4H, SO$_3$H), 8.11–8.33 (4H, Ar-H), 7.63–7.90 (8H, Ar-H). δ_P ((CD$_3$)$_2$SO) −201.50. m/z (MALDI-TOF) 882.80 [M$^+$].

Photophysical Measurements

UV/Vis absorption measurements were made with either a HP 8451A or a Hitachi spectrophotometer in 10 mm quartz cuvettes. Fluorescence spectra up to 900 nm were monitored using a Perkin–Elmer LS 55. All spectra were corrected for the sensitivity of the photomultiplier tube. The fluorescence quantum yield (Φ_f) was calculated by $\Phi_f = F_s A_0 \Phi_f^0/(F_0 A_s)$ and measured relative to ZnPc in DMF ($\Phi_f^0 = 0.30$).[20] A wavelength of 610 nm that corresponded to S$_1$ excitation was employed. The sample and reference solutions were prepared with the same absorbance (A_i) at the excitation wavelength (near 0.09 per cm). All solutions were air saturated. Fluorescence lifetime (τ_f) was measured by a time-correlated single photon counting method (Edinburgh FL-900 spectrophotometer) with excitation at 650 nm either by a 50 ps CdS portable diode laser or a hydrogen nanosecond flash lamp, the emission was monitored at 700 nm. Measurements were carried out at room temperature of 22°C.

Transient absorption spectra were recorded in de-aerated DMF (prepared by bubbling argon for 15 min) with an Edinburgh LP-920 laser flash photolysis system. A Nd:YAG laser (Continuum surelite II, 355 nm and 7 ns FWHM) was used as the excitation source. The analyzing light was from a xenon lamp. The laser and analyzing light beams perpendicularly passed through a quartz cell with an optical path length of 1 cm. The signal was displayed and recorded on a Tektronix TDS 3012B oscilloscope and an Edinburgh LP900 detector. The laser energy incident at the sample was attenuated to a few mJ per pulse. Time profiles at a series of wavelengths from which point-by-point spectra were assembled and recorded with the aid of a PC

controlled kinetic absorption spectrometer. The concentrations of the target compounds were typically 10×10^{-6} M providing $A_{355} = 0.20$ in a 10 mm cuvette.

The triplet–triplet absorption coefficients (ε_T) of the samples were obtained using the singlet depletion method,[21] and the following equation was used to calculate the ε_T

$$\varepsilon_T = \varepsilon_S \frac{\Delta OD_T}{\Delta OD_S},\qquad(2)$$

where ΔOD_S and ΔOD_T are the absorbance change of the triplet transient difference absorption spectrum at the minimum of the bleaching band and the maximum of the positive band, respectively, and ε_S is the ground-state molar absorption coefficient at the UV-vis absorption band maximum. Both ΔOD_S and ΔOD_T were obtained from the triplet transient difference absorption spectra.

The triplet quantum yield Φ_T was obtained by comparing the ΔOD of the optically matched sample solution at 355 nm in a 1 cm cuvette to that of the reference, ZnPc ($\Phi_T = 0.65 \pm 0.02$, $\varepsilon_{480} = 30\,000 \pm 1000$ M^{-1} cm^{-1}),[22] using the equation[23]

$$\Phi_T = \Phi_T^{ZnPc} \frac{\Delta OD_T}{\Delta OD_T^{ZnPc}} \frac{\varepsilon_T^{ZnPc}}{\varepsilon_T},\qquad(3)$$

where the superscripts represents the reference, ΔOD is the absorbance of the triplet transient difference absorption spectrum at the selected wavelength, and ε_T is the triplet excited-state molar absorption coefficient.

Singlet oxygen quantum yield (Φ_Δ) determinations were carried out using the chemical trapping method.[24] Typically, a 2 mL portion of the respective PTBC solutions that contained diphenylbenzofuran (DPBF) was irradiated at 670 nm in air-saturated dimethyl sufoxide (DMSO). Φ_Δ values were obtained by the relative method using ZnPc as the reference (Eqn 4):

$$\Phi_\Delta = \Phi_\Delta^{ref} \frac{k}{k^{ref}} \frac{I_a^{ref}}{I_a},\qquad(4)$$

where Φ_Δ^{ref} is the singlet oxygen quantum yield for the standard (0.65 for ZnPc in DMSO),[25] k and k^{ref} are the DPBF photobleaching rates in the presence of the respective samples and standard, respectively; I_a and I_a^{ref} are the rates of light absorption at the irradiation wavelength of 670 nm by the samples and standard, respectively. Their ratio can be obtained by Eqn 5.

$$\frac{I}{I_a^{ref}} = \frac{1 - 10^{-A_{670}}}{1 - 10^{-A_{670}^{ref}}}.\qquad(5)$$

To avoid chain reactions induced by DPBF in the presence of singlet oxygen, the concentration of DPBF was lowered to $\sim3 \times 10^{-5}$ mol dm^{-3}. A solution of sensitizer (absorbance ~0.65 at the irradiation wavelength) that contained DPBF was prepared in the dark and irradiated in the Q-band region. DPBF degradation at 415 nm was monitored. The error in the determination of Φ_Δ was $\sim10\%$ (determined from several Φ_Δ values).

References

[1] I. Aviv, Z. Gross, *Chem. Commun.* **2007**, 1987. doi:10.1039/B618482K

[2] R. Paolesse, S. Nardis, F. Sagone, R. G. Khoury, *J. Org. Chem.* **2001**, *66*, 550. doi:10.1021/JO005661T

[3] Z. Gross, N. Galili, I. Saltsman, *Angew. Chem. Int. Ed.* **1999**, *38*, 1427. doi:10.1002/(SICI)1521-3773(19990517)38:10<1427::AID-ANIE1427>3.0.CO;2-1

[4] R. Paolesse, L. Jaquinod, D. J. Nurco, S. Mini, F. Sagone, T. Boschi, K. M. Smith, *Chem. Commun.* **1999**, 1307. doi:10.1039/A903247I

[5] D. T. Gryko, *Eur. J. Org. Chem.* **2002**, 1735. doi:10.1002/1099-0690(200206)2002:11<1735::AID-EJOC1735>3.0.CO;2-K

[6] M. Gouterman, P. Sayer, E. Shankland, J. P. Smith, *Inorg. Chem.* **1981**, *20*, 87. doi:10.1021/IC50215A021

[7] M. Fujiki, H. Tabei, K. Isas, *J. Am. Chem. Soc.* **1986**, *108*, 1532. doi:10.1021/JA00267A024

[8] J. Liu, F. Zhang, F. Zhao, Y. Tang, X. Song, G. Yao, *J. Photochem. Photobiol. Chem.* **1995**, *91*, 99. doi:10.1016/1010-6030(95)04102-L

[9] J. Liu, Y. Zhao, F. Zhao, F. Zhang, X. Song, F. T. Chau, *J. Photochem. Photobiol. Chem.* **1996**, *99*, 115. doi:10.1016/S1010-6030(96)04385-7

[10] J. Liu, F. Zhang, F. Zhao, Y. Tang, X. Song, *J. Photochem. Photobiol. Chem.* **1999**, *124*, 165. doi:10.1016/S1010-6030(99)00107-0

[11] J. Li, L. R. Subramanian, M. Hanack, *Eur. J. Org. Chem.* **1998**, 2759. doi:10.1002/(SICI)1099-0690(199812)1998:12<2759::AID-EJOC2759>3.0.CO;2-9

[12] J. Li, L. R. Subramanian, M. Hanack, *Chem. Commun.* **1997**, 679. doi:10.1039/A700532F

[13] J. P. Fox, D. P. Goldberg, *Inorg. Chem.* **2003**, *42*, 8181. doi:10.1021/IC034792K

[14] L. Huang, C. Zhong, F. Zhang, C. H. Tung, *Bioorg. Med. Chem. Lett.* **2008**, *18*, 2152. doi:10.1016/J.BMCL.2008.01.111

[15] M. Klessinger, in *Excited States and Photochemistry of Organic Molecules* (Eds M. Klessinger, J. Michl) **1995**, p. 63 (VCH: New York, NY).

[16] N. Kobayashi, F. Furuya, G.-C. Yug, H. Akita, M. Yokomizo, N. Ishikawa, *Chem. Eur. J.* **2002**, *8*, 1474. doi:10.1002/1521-3765(20020315)8:6<1474::AID-CHEM1474>3.0.CO;2-P

[17] C. Reichardt, in *Solvents and Solvent Effects in Organic Chemistry* (Ed. C. Reichardt) **2003**, p. 329 (Wiley-VCH: Weinheim).

[18] X.-F. Zhang, H. Xu, *J. Chem. Soc., Faraday Trans.* **1993**, *89*, 3347. doi:10.1039/FT9938903347

[19] X.-F. Zhang, H. Xu, *Chem. Res. Chin. Univ.* **1994**, *15*, 917.

[20] P. G. Seybold, M. Gouterman, *J. Mol. Spectrosc.* **1969**, *31*, 1. doi:10.1016/0022-2852(69)90335-X

[21] I. Carmichael, L. H. Gordon, *J. Phys. Chem. Ref. Data* **1986**, *15*, 1.

[22] T. H. Tran Thi, C. Desforge, C. Thiec, S. Gaspard, *J. Phys. Chem.* **1989**, *93*, 1226. doi:10.1021/J100341A013

[23] C. V. Kumar, L. Qin, P. K. Das, *J. Chem. Soc., Faraday Trans.* **1984**, *280*, 783.

[24] M. G. Lagorio, L. E. Dicelio, E. A. S. Roman, S. E. Braslavsky, *J. Photochem. Photobiol. B* **1989**, *3*, 615. doi:10.1016/1011-1344(89)80084-3

[25] N. Kuznetsova, N. Gretsova, E. Kalmykova, E. Makarova, S. Dashkevich, V. Negrimovskii, O. Kaliya, E. Luk'yanets, *Russ. J. Gen. Chem.* **2000**, *70*, 133.